

Process Modeling and Optimization of Resistance Welding for Thermoplastic Composites

ZIYA SEYHAN COLAK, FAZIL ONDER SONMEZ* AND
VAHAN KALENDEROGLU

*Department of Mechanical Engineering
Bogazici University
Istanbul, Bebek, 80815
Turkey*

(Received March 14, 2000)
(Revised January 25, 2001)

ABSTRACT: Resistance welding is a suitable technique for joining thermoplastic composites. Like other fusion bonding processes, it involves heating, melting and cooling steps. Productivity depends on the time that passes during these steps. This is the first study that tries to increase the productivity of the process in a systematic way. The objective of the present study is to determine the optimum set of process parameters to minimize the processing time. In order to ensure that the resulting joint satisfied the requirements of quality, the relationship between process variables and quality of the welded joint was established through process modeling. First, a one-dimensional transient heat transfer analysis was carried out using a finite difference method to find the temperature profiles across the thickness of the welding stack. Then, the heat transfer analysis was coupled with a degradation kinetics model in order to determine whether the resulting part has undergone excessive thermal degradation, or not. Finally, a bonding model adapted to the resistance welding process was used to determine the degree of bonding between the laminates. The process model was eventually combined with an optimization algorithm to minimize the processing time without violating the quality requirements. The algorithm was based on a search method called Nelder–Mead. Finally, optimum process parameters were obtained for different thicknesses of APC-2 laminates.

INTRODUCTION

FIBER REINFORCED THERMOPLASTIC composites have been introduced as structural materials for high performance applications as an alternative to thermoset composites. Because of the limited deformation capacity of continuous fiber reinforcements, only

*Author to whom correspondence should be addressed.

structures having relatively simple geometry can effectively be produced from these materials in order to conserve the potential for rapid and low-cost production. In order to create large and complex structures, several of these simple components must be joined together. The thermoplastic matrix in such composites enables the application of fusion bonding techniques to replace the traditional joining methods such as adhesive bonding and mechanical fastening.

Fusion bonding is accomplished by raising the temperature of the joint above the melt temperature of the thermoplastic polymer at the interface, and then allowing the joint to cool down while intimate contact is maintained by the applied pressure [1]. The advantages of fusion bonding over other joining techniques include the elimination of stress concentrations and damaging of fibers, which is inevitable in mechanical fastening, and the possibility of achieving bond performance similar to the bulk properties of the joined parts. The processing times for welding are much shorter than those involved in adhesive bonding which requires extensive surface preparation [2]. It also offers the chance of reprocessing if inspection shows that bonding is not complete.

Fusion bonding can be performed by supplying heat to the system, which can be achieved in a number of ways. Resistance welding is a simple way of generating heat. By passing an electric current through the carbon fibers of a ply, sandwiched between two thermoplastic composite laminates, fusion bonding can be achieved quickly (Figure 1). To accomplish this, a single unidirectional carbon fiber prepreg with a thermoplastic matrix is used as the resistance heating element [1]. Since the heating element will become part of the bond, it must be compatible with the matrix of the composite laminates to be joined. Yet, the range of compatible materials seems to be large. Indeed, use of a steel mesh as heating element was reported to produce strong joints [3]. The inclusion of a thin thermoplastic film between the heating element and the laminate was recommended, in order to give a

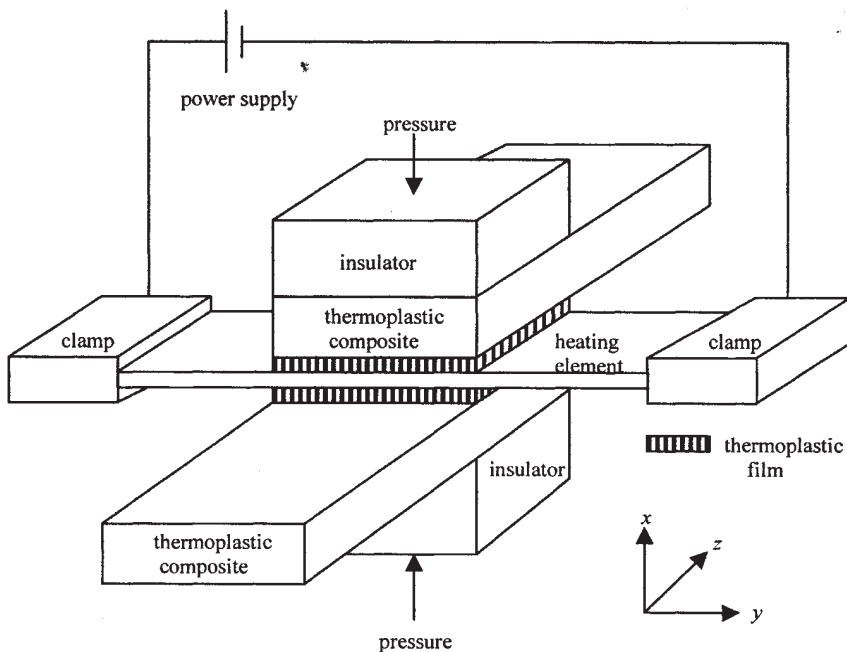


Figure 1. Resistance welding setup for joining thermoplastic composites [2,5].

degree of resin richness that facilitates the welding process [4]. A plate is used for the purpose of insulating the parts to be joined and creating a uniform pressure.

During the welding process, the electrical heating must be sufficient to melt the thermoplastic matrix of the single ply, the thermoplastic film and the thermoplastic matrix on the inner surfaces of the laminates. If the supplied thermal energy exceeds the heat loss from the joint, temperature increases, and thus melting and fusion of the interface take place. The current is switched off after nominal melting of the interface is achieved, and the joint is allowed to cool down, while consolidation pressure is maintained [1]. The consolidation pressure impedes the void growth, and sustains the intimate contact.

Resistance welding has been studied by several research groups in recent years. Benatar and Gutowski [6] investigated a variety of methods for joining advanced thermoplastic composites, including resistance welding. They found the resistance welding process to be one of the most successful bonding techniques. Eveno and Gillespie [7] investigated experimentally resistance welding of preconsolidated unidirectional graphite (AS4) reinforced polyetheretherketone (PEEK) composite laminates (APC-2). They conducted experiments to identify important process variables governing the efficiency of the welding process. Maffezzoli et al. [8] developed a mathematical model in order to describe the welding behavior of APC-2 laminates. By using the model, they determined the temperature and crystallinity profiles along the thickness of the welding system. Jakobsen et al. [9] developed a transient two-dimensional anisotropic thermal model of the resistance welding process for semicrystalline thermoplastic composites. They investigated resistance-welded double cantilever beam specimens made of unidirectional graphite-reinforced-polyetheretherketone plies. Bastien and Gillespie [10] studied the non-isothermal fusion bonding of thermoplastic composites (graphite/PEEK) using an amorphous film (PEI) at the interface. They proposed a model, based on the healing theory of amorphous polymers to predict strength and toughness as a function of non-isothermal process history. Holmes and Gillespie [11] developed one-dimensional and two-dimensional thermal models for large-scale sequential resistance welding processes. They conducted a parametric study to investigate the influence of welding parameters. Don et al. [1,12] performed extensive experimental work to find lap-shear strength and interlaminar fracture toughness of resistance-welded APC-2 laminates in both unidirectional and quasi-isotropic configurations, using PEEK and polyetherimide (PEI) films at the joint interface. Hou et al. [13] experimentally investigated resistance welding of CF-fabric/PEI composites and developed a processing window using power level and heating time as process variables. Xiao et al. [5] considered the use of resistance welding for the purpose of repairing thermoplastic composite structures and examined different fusion bonding techniques. They also developed a two-dimensional finite element model for resistance welding of APC-2 lap-shear specimens. Ageorges et al. [2] proposed a transient three-dimensional finite element model for resistance welding of thermoplastic composite lap-shear specimens. Later, they extended their work on resistance welding by modeling consolidation and crystallization [14,15]. They also evaluated different welding configurations for lap-shear specimens, namely APC-2 laminate/PEEK film, APC-2 laminate/PEI film and CF-PEI laminate/PEI film.

Model-based analyses and experimental studies of the resistance welding process were carried out in the previous studies. Parametric studies or experimentation were the usual methods for determining a suitable set of process parameters. However, the problem of determining the processing conditions in which one can achieve the process in the shortest possible time without compromising the quality of the resulting joint has not been

attacked so far. The objective of the present study is to create a process model for resistance welding and obtain the optimum set of process parameters that minimizes the processing time. Requirements of full consolidation and limited thermal degradation constitute the constraints of the optimization problem. In order to produce a joint with the desired properties, one should compromise two contradictory effects. Supplying a larger amount of heat results in higher temperature levels and thus facilitates consolidation but also accelerates degradation. On the other hand, if one chooses a smaller amount of heat, consolidation is adversely affected but degradation becomes less severe. Therefore, consolidation and degradation set the lower and upper limits on the amount of the heat supplied. Since thermal degradation and consolidation depend on the temperature during the process, a one-dimensional transient heat transfer analysis was carried out using a finite difference method which gave the temperature profiles across the thickness of the welding stack. Then, the heat transfer analysis was coupled with a degradation kinetics model in order to determine whether or not the resulting part has undergone excessive thermal degradation. Finally, a bonding model adapted to the resistance welding process was used to determine the degree of bonding between the laminates.

Since the effects of process parameters on the quality of the joint interact with each other, a parametric study is not feasible for this problem. Therefore, the use of an optimization algorithm is needed. Accordingly, the process model was combined with an optimization algorithm to obtain the optimum process state, which minimized the processing time without violating quality constraints, and thus achieving high productivity. The process state was defined in terms of the power input and the heating time during which the power is applied.

THE HEAT TRANSFER ANALYSIS

In this study, we assume that heat loss predominantly occurs through the top and bottom surfaces of the composite. The results of the previously reported two- and three-dimensional thermal models of Xiao et al. [5] and Ageorges et al. [2], respectively, did not show any significant change in temperature along the length and width of the composite, in comparison with the temperature variation across the thickness. Therefore, these studies support our assumption. The problem is thus reduced to that of one-dimensional transient heat transfer across the thickness of the composite. The governing equation can then be written as

$$\frac{\partial}{\partial X} \left(k \frac{\partial T}{\partial X} \right) + \dot{q} = \rho c \frac{\partial T}{\partial t} \quad (1)$$

where k , ρ , c and \dot{q} are thermal conductivity, density, specific heat and heat generation rate per unit volume, respectively. The symmetry of the welding system about the y - z plane (Figure 1) implies that heat transfer does not occur through that plane, and thus it can be considered as an insulated surface (Figure 2).

The boundary condition at $x = 0$ therefore becomes

$$\frac{\partial T(0, t)}{\partial x} = 0 \quad (2)$$

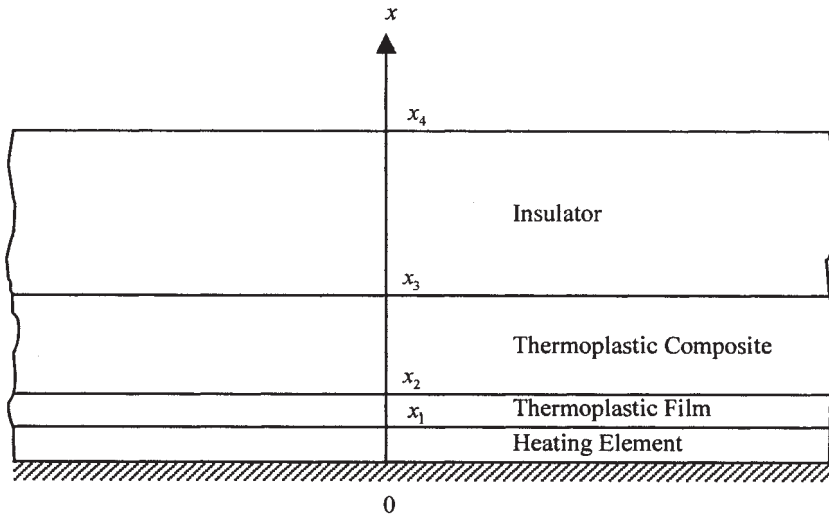


Figure 2. Schematic of the one-dimensional modeling case.

The outer boundary surface at $x = x_4$, dissipates heat by convection to the surrounding air. If the ambient temperature is T_∞ the following boundary condition holds on the top:

$$-k_4 \frac{\partial T(x_4, t)}{\partial x} = h[T(x_4, t) - T_\infty] \tag{3}$$

where k_4 is the thermal conductivity of the insulator; and h is the heat transfer coefficient on the top surface.

In the model, it is assumed that heat is directly conducted between individual layers of the welding stack, which is true only when full intimate contact is achieved. To simulate imperfect intimate contact, a gap conductance term may be introduced to account for the partial contact at the interfaces. However, Ageorges et al. [2] observed that introducing the gap conductance concept to simulate the presence of rough contact surfaces between the heating element, the neat thermoplastic film and the thermoplastic composite laminate does not affect the predictions significantly. These observations thus validate the perfect intimate contact assumption. For the other interface at $x = x_3$, the same assumption can be made.

The interface conditions can then be expressed as

$$T(x_{m^-}, t) = T(x_{m^+}, t) \quad m = 1, 2, 3 \tag{4}$$

$$k_m \frac{\partial T(x_{m^-}, t)}{\partial x} = k_{m+1} \frac{\partial T(x_{m^+}, t)}{\partial x} \quad m = 1, 2, 3 \tag{5}$$

Considering that polymer properties are quite sensitive to the change in temperature, and joining operation requires considerable temperature change from the room temperature to above the melting temperature, thermal properties may not be assumed to be constant during the process. Therefore, in order to determine the temperature field accurately, temperature-dependent material properties should be used. In this study,

the temperature-dependent material properties, reported by Ageorges et al. [2] for PEEK and APC-2, are used.

The transient thermal analysis becomes non-linear if the material properties are assumed to be temperature-dependent. Because of the non-linearity caused by the assumption of a variable thermal conductivity, we cannot apply an analytical method to solve the governing differential equations. For this reason, we employed the Crank–Nicolson scheme to solve the transient heat conduction problem, which is an implicit method. An explicit method was not used to avoid the restriction imposed by the stability requirement on the size of the time increment. The resulting finite difference equation can be expressed as [16]

$$\frac{1}{2} \left[\frac{(k_{i-1} + k_i/2)(T_{i-1}^{n+1} - T_i^{n+1}) - (k_i + k_{i+1}/2)(T_i^{n+1} - T_{i+1}^{n+1})}{(\Delta x)^2} + \frac{(k_{i-1} + k_i/2)(T_{i-1}^n - T_i^n) - (k_i + k_{i+1}/2)(T_i^n - T_{i+1}^n)}{(\Delta x)^2} \right] + \dot{q} = \rho_i c_i \frac{T_i^{n+1} - T_i^n}{\Delta t} \quad (6)$$

where the subscripts $(i - 1)$, (i) and $(i + 1)$ represent the nodal points in the direction; the superscripts (n) and $(n + 1)$ represent conditions at times (t) and $(t + \Delta t)$; Δx represents the step size in length; and represents the size of the time increment. Özisik [16] used the method of lagging the evaluation of the temperature- dependent properties by one time step, in order to write Equation (6).

Heat Generation

In a resistance welding process, the heat generation per unit volume within the solution domain can be expressed as [9]

$$\dot{q} = \begin{cases} \dot{q}_{\text{elec}} + \dot{q}_{\text{crys}} - \dot{q}_{\text{melt}} & 0 \leq x < x_1 \\ \dot{q}_{\text{crys}} - \dot{q}_{\text{melt}} & x_1 \leq x < x_3 \\ 0 & x_3 \leq x < x_4 \end{cases} \quad (7)$$

where \dot{q}_{elec} is the rate at which electrical energy is generated per unit volume; \dot{q}_{melt} is the rate at which energy is absorbed per unit volume during melting of the crystals; and \dot{q}_{crys} is the rate at which energy is released per unit volume during the crystallization of the thermoplastic matrix. The effect of latent heat resulting from crystallization and melting of crystals on the heat transfer, appears to be very small as compared to \dot{q}_{elec} and thus is negligible [9,15]. The energy corresponding to latent heat is only of the order of a few percent of the total electrical energy supplied to the heating element. Therefore, \dot{q}_{melt} and \dot{q}_{crys} in Equation (7) are neglected. The electrically generated \dot{q}_{elec} is related to the resistance, R , of the heating element. The resistance of the heating element is very critical to the welding process and can be found from the following expression [9]:

$$R = \gamma \frac{1}{w} \quad (8)$$

where γ is the resistivity per thickness of the rectangular heating element (Ω) of length l and width w . The APC-2 prepreg heating elements have an average resistivity, γ , of 0.175 Ω per prepreg thickness [5]. The electrical power is supplied through the heating element. The power delivered is simply

$$P = UI = I^2 R \quad (9)$$

where U is the voltage; and I is the applied current. The volumetric heat generation rate, \dot{q}_{elec} , can then be expressed as

$$\dot{q}_{\text{elec}} = \frac{P}{V} = \frac{I^2 R}{V} \quad (10)$$

where V is the volume of the heating element:

$$V = lwh \quad (11)$$

where h is the thickness of the heating element. From Equations (8) to (11), the following equation is obtained:

$$\dot{q}_{\text{elec}} = \left(\frac{I}{w}\right)^2 \frac{\gamma}{h} \quad (12)$$

THE DEGRADATION ANALYSIS

When a polymer is exposed to high temperatures, it tends to degrade and decompose because of unstable or reactive condition of covalent bonds. Day et al. [17] suggested that the degradation of PEEK in air is dependent on both the rate of oxygen diffusion to the polymer and the rate of volatilization of degraded fragments. The controlling mechanism of degradation in air is, therefore, the transport of oxygen through the melt. In the resistance welding process, the maximum temperature occurs at the center of the heating element. Thus, the start of serious degradation can be checked by calculating the amount of degradation at the center of the heating element. Since it has no contact with the surrounding air, a degradation kinetics model, which was developed in nitrogen atmosphere, can be applied to the resistance welding process without much compromise of the accuracy of the results.

Thermal degradation, as considered in this study, pertains to the material weight loss of the thermoplastic matrix. While other chemical mechanisms like cross-linking may additionally affect the properties and the overall performance of the composite, the material weight loss has been the principal measure of degradation modeled in the literature [18]. The amount of degradation α_d is given by the ratio of the current weight loss to the final weight loss:

$$\alpha_d = \frac{M_0 - M}{M_0 - M_f} \quad (13)$$

where M , M_0 and M_f are the current, initial and final weights of the polymer, respectively. Nam and Seferis [19] developed a non-isothermal model to describe the polymer weight loss caused by thermal degradation. Their model was applicable to PEEK in a nitrogen atmosphere, and the rate of change in weight loss was given by

$$\frac{d\alpha_d}{dt} = k(T)f(\alpha_d) \quad (14)$$

where $k(T)$ is a rate constant and $f(\alpha_d)$ is the degradation factor. The temperature dependence of the rate constant was described by an Arrhenius expression:

$$k(T) = A \exp\left(-\frac{E}{RT}\right) \quad (15)$$

where A is a pre-exponential factor and for PEEK it is equal to $8.265 \times 10^{12} \text{ s}^{-1}$ [19]; E is the activation energy and for PEEK it is equal to $240.2 \times 10^3 \text{ J/mol}$ [19]; and $R = 8.3145 \text{ J/mol K}$ is the universal gas constant. For PEEK, the degradation factor $f(\alpha_d)$ can be expressed as

$$f(\alpha_d) = w_1(1 - \alpha_d) + w_2\alpha_d(1 - \alpha_d) \quad (16)$$

where $w_1 = 0.0215$ and $w_2 = 0.9785$ are the weight factors [19]. Nam and Seferis considered 36% of the original weight as the main weight loss capacity of PEEK. The percentage of reduction in the weight of the polymer is then expressed as

$$\alpha = 100 \frac{M_0 - M}{M_0} = 36\alpha_d \quad (17)$$

THE CONSOLIDATION ANALYSIS

Consolidation in a composite manufacturing process is accomplished by applying pressure and heat to the material system to squeeze out the air and volatiles, or melt them within the material. Incomplete consolidation results in high void content, which may seriously degrade inter-laminar shear strength of the composite, which has a significant effect on compressive strength, impact resistance and fatigue life [20]. Therefore, accurate modeling of the consolidation process plays an important role in ensuring the quality of the resulting composite structure. In resistance welding, consolidation can be characterized by a polymer to polymer interface healing process [14], which involves diffusion of polymer chains through the interface. The establishment of intimate contact is requisite for the development of autohesion.

Intimate Contact

Loos and Dara [21] developed a model to describe the development of intimate contact and bond formation between plies during processing of amorphous thermoplastic

composites. They assumed that irregular surfaces of the plies can be represented by a wave of rectangular elements having different sizes and analyzed the behavior of these elements. Lee and Springer [22] proposed a model for intimate contact based on the work of Loos and Dara for processing of thermoplastic composites. They followed the model of Loos and Dara but considered the elements of the same size. Mantell and Springer [23] adapted the model developed by Lee and Springer to tape laying and filament winding processes. Since these are non-isothermal processes, their model is also suitable for resistance welding. The expression for the degree of intimate contact was given as [23]:

$$D_{ic}(t) = a^* \left[\int_0^t \frac{P_{app}}{\mu_{mf}} d\tau \right] \quad (18)$$

where P_{app} is the applied pressure. To prevent void formation, this consolidation pressure should be applied until the maximum temperature in the welding stack becomes lower than 143°C, which corresponds to the glass transition temperature of PEEK matrix. In contrast to tape laying, in resistance welding the pressure is uniform. Therefore, it was kept constant during the simulation. The geometric factor a^* can be determined by fitting the model to the experimental data. Ageorges et al. [14] determined a^* to be 0.147 for the interface between APC-2 laminate and PEEK film. This value was also used in the present study in order to calculate the effect of surface roughness on consolidation. The viscosity of the material, μ_{mf} , was assumed to be temperature-dependent. For the APC-2 matrix-fiber system, viscosity is expressed as [23]

$$\mu_{mf} = 132.95 \exp\left(\frac{2969}{T}\right) \quad (19)$$

where the temperature T is given in K.

Autohesion

Once two surfaces are brought into intimate contact and, thus, the physical barrier between the two surfaces is removed, molecules are free to move across the interface in the so-called autohesion process [14]. Diffusion of macromolecules across the interface starts because of random thermal motions. After sufficient time has passed, some of the chains will have diffused across the interface and entangled with molecular chains on the other side of the interface, so that interface is no longer distinguishable from the bulk polymer. The development of autohesion can be described by the reptation theory which was first developed by de Gennes [24]. The reptation theory is suitable to describe the motion of a chain at the interface. The theory was successfully applied by Wool et al. [25,26] for the prediction of mechanical properties during healing. Cho and Kardos [27] performed isothermal experiments for PEEK and confirmed Wool's findings. Bastien and Gillespie [10] applied the reptation theory to resistance welding of APC-2 laminates using a PEI film. Sonmez and Hahn [28] modified the reptation model of de Gennes in order to simulate autohesion under non-isothermal process conditions for thermoplastic composite tape placement. Ageorges et al. [14] used a model for autohesion based on the work of Bastien and Gillespie for the resistance welding of thermoplastic-matrix composite lap-shear specimens.

Diffusion of molecular chains across an interface is a temperature-driven process. In order to consider non-isothermal processes, the temperature history is divided into finite time intervals during which the temperature is assumed to be constant. This is an approach similar to that of Bastien and Gillespie [10]. In each isothermal step, the healing theory can then be applied. The resulting expression is as follows [28,29]:

$$D_{au}(t) = \left[\int_0^i \frac{d\tau}{2\sqrt{\tau t_r(\tau)}} \right]^{1/2} \quad (20)$$

where the reptation time t_r is related to the temperature through an Arrhenius law:

$$t_r = C \exp \left[\frac{R_\alpha}{R} \left(\frac{1}{T} - \frac{1}{T_{ref}} \right) \right] \quad (21)$$

where the following values for the above constants apply for PEEK: C is the parameter for the reptation time and is equal to 0.11 sec [30]; E_a is the activation energy of diffusion of the polymer and is equal to 57300 [30]; T_{ref} is the reference temperature and is equal to 673.15 [30]; T is the inter-ply temperature; and R is the universal gas constant.

Degree of Bond

In general, the processes of intimate contact and autohesion are coupled, in that intimate contact is a prerequisite for the initiation of autohesion. Once intimate contact is established at a point along the interface, autohesion, and thus bonding process starts. The area that is in contact increases with time. The degree of bond D_b can be defined as the area average of bond strengths calculated for each of the incremental areas that come into intimate contact throughout the duration of the bonding process. Considering a time interval between τ and $\tau + \Delta\tau$ during the process, the incremental dimensionless area that comes into intimate contact in this period is given by $(dD_{ic}/d\tau)d\tau$. The extent of autohesion for this incremental area, observed at a final time t_b , may be denoted as $D_{au}(t_b - \tau)$, where $t_b - \tau$ is the time available for the incremental area to heal. The net bond strength developed at the interface after a time t_b is an area average of the bond strengths of each of the incremental areas. The degree of bond D_b may be expressed in a dimensionless form as follows [30]:

$$D_b(t_b) = \int_0^{t_b} D_{au}(t_b - \tau) \frac{dD_{ic}(\tau)}{d\tau} d\tau \quad (22)$$

where t_b is the duration of the process. Bonding is complete when D_b becomes unity.

PROCESS WINDOW DEVELOPMENT

The ultimate goal of the process modeling for resistance welding is to quantify the process parameters that will result in a joint satisfying the quality requirements. A process window is defined by feasible ranges of values of process parameters that result in joints

with desired properties. In this study, a process window for resistance welding is developed using weight loss through thermal degradation and interlaminar shear strength as product quality criteria. Previously described analyses for heat transfer, degradation and consolidation are combined to build the process window for resistance welding.

As the first quality requirement, the extent of thermal degradation of the material should not be excessive so that its effect on the overall performance of the composite part is negligible. As mentioned previously, thermal degradation of the polymer results from prolonged exposure of the laminates to high temperatures during the process, which in turn degrades the properties and performance of the products. Among its effects are the loss in the material modulus, and the increase in the glass transition temperature of the polymer [18]. The increase in the glass transition temperature may significantly affect the bonding of the layers and the final strength of the product. It is therefore important to ensure that the amount of degradation remains within allowable limits. Cogswell [31] suggested the maximum process times at different processing temperatures for APC-2 in an oxygen-free environment. Sonmez and Hahn [32] compared the results of the degradation kinetics model of Nam and Seferis [19] to the data given by Cogswell [31]. In their work [32], they estimated the maximum allowable weight loss to be 0.01%, which fully satisfied the suggested maximum process times given by Cogswell [31].

The objective in resistance welding is to fully achieve consolidation during the joining process, so that bulk properties are realized at the joint. The resulting void content in the composite is an important parameter affecting the product quality. Voids may alter the mechanical and thermal properties of the composite considerably, as well as initiate and accelerate material failure mechanisms [18]. Furthermore, the presence of voids reduces load-carrying capacity of the laminate.

Although the process pressure favorably affects the development of intimate contact, excessive process pressures should be avoided because of possible fiber damage, fiber-bed spread or resin starvation. Xiao et al. [5] conducted experiments to compare the lap-shear strengths and the void contents of APC-2 specimens welded by resistance welding under different pressures. In their work, they observed experimentally that a pressure as low as 1.2 was sufficient to prevent deconsolidation of APC-2 laminates during resistance welding. In this study, as in some previous studies [1,12,14], the welding pressure is taken as 1.38 MPa.

In the process model (Figure 3), the degree of bond was calculated at the interface between the PEEK film and the APC-2 laminate. This is because this interface experiences a lower temperature compared to the interface between the heating element and the PEEK film and accordingly, a lower degree of bonding is expected.

The bonding process continues as long as the temperature is high enough to allow molecular mobility. Cho and Kardos [27] reported that bonding below 270°C was very slow. Accordingly, bonding calculations are continued as long as the temperature at the interface is above 270°C.

Because of the restricted movement of crystallized polymer chains, the autohesion process starts at temperatures above 320°C, which corresponds to the transition temperature between crystallization and melting [33]. During cooling, crystallization starts at about 320°C, but it takes time to complete. Therefore, autohesion calculations are continued until 270°C.

The process time t_w is the time that passes between the onset of power delivery and cooling below the glass transition temperature. During this time, pressure and thus intimate contact is maintained.

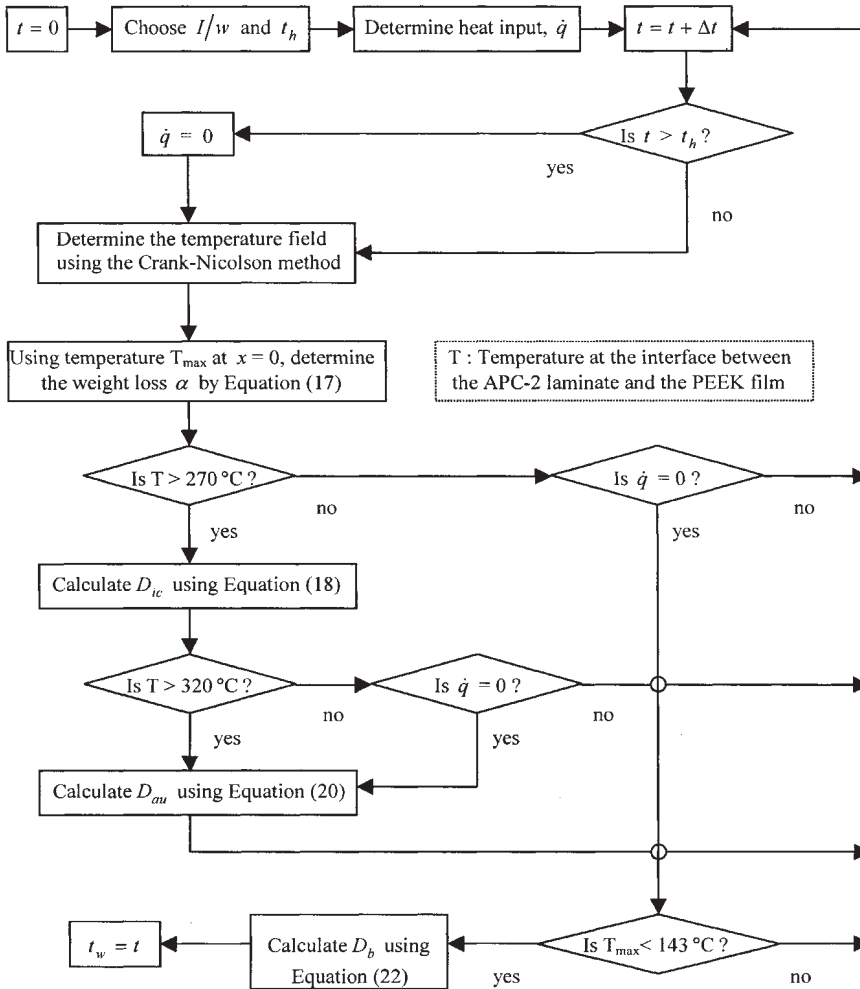


Figure 3. Solution procedure in the process model for resistance welding. t_h is the welding time and I/w is the current intensity per unit width.

The process model is used in order to calculate some input parameters for the optimization procedure. These input parameters are the weight loss through thermal degradation α , degree of bonding D_b and welding (process) time t_w .

OPTIMIZATION

The purpose of optimization is to find the best possible solution among the many potential solutions for the given problem in terms of a performance criterion. The objective of the process optimization problem for resistance welding is to minimize the process time without violating the product quality constraints. Processing times can be reduced by increasing the power input as much as possible without violating the constraints. Since our process modeling is based on a numerical method, it is difficult to

use the optimization algorithms that require the derivative of the objective and the constraint functions. In this respect, zero order methods are more suitable. Among them are stochastic and deterministic methods. The advantage of stochastic methods like Simulated Annealing and Genetic Algorithms is that they may easily converge to the global minimum and start from any set of values of process parameters whether it is satisfying the constraints, or not. However, they are difficult to apply and expensive in terms of computational time. Zero order deterministic methods like Nelder–Mead and Powell's methods are much easier to apply but they do not necessarily converge to the global optimum. A deterministic algorithm should be employed many times starting from different points within the feasible region of process parameters. Then, the lowest value is chosen as the global minimum of the objective function. In this study, the search for optimum process parameters was started with the use of the Nelder–Mead method [34]. Using this method, the solution domain was proven to be containing a low number of local minima. Therefore, the Nelder–Mead method was found to be a suitable choice.

Polymer Degradation Constraint

The degradation in this study is quantified as the material weight loss during the process. This constraint may be written as an inequality relationship of the form

$$\alpha \leq \alpha_{\max} \quad (23)$$

where α is the degree of degradation at the center of the heating element, the location where the temperature is highest during the welding process; and α_{\max} is the maximum allowable degree of degradation, which is 0.01% polymer weight loss, as mentioned before. Equation (17) is used to calculate α .

Interlaminar Shear Strength Constraint

Shear strength at the joint is supposed to reach its ultimate value or, equivalently, the degree of bond, D_b , should reach unity, i.e. complete interfacial bonding should be achieved:

$$\sigma = \sigma_{\infty} \quad \text{or} \quad D_b = 1 \quad (24)$$

Since a relationship has already been established between the shear strength σ and the degree of bond D_b , only the degree of bond will be considered. For full consolidation, the interface between the APC-2 laminate and the neat PEEK film should have $D_b = 1$ at the end of the welding process.

Objective Function

Since two quality criteria (Equations 23 and 24) should be satisfied in the resulting joint, our problem is a constrained optimization problem in which degradation and consolidation act as constraints. However, by using penalty functions, a constrained optimization problem can be transformed into an unconstrained problem. As a result,

much simpler algorithms can be employed for the minimization such as the one that we use. A combined objective function may be constructed [35] with the aforementioned constraints (Equations 23 and 24):

$$f = \frac{t_w}{t_{\max}} + C_1(1 - D_b)^2 + C_2(\alpha - \alpha_{\max})^2, \quad (\alpha - \alpha_{\max}) = \begin{cases} 0 & \text{for } \alpha \leq \alpha_{\max} \\ \alpha - \alpha_{\max} & \text{for } \alpha > \alpha_{\max} \end{cases} \quad (25)$$

where t_w is the welding (process) time, which is normalized by a maximum time, ($t_{\max} = 1000$ s); C_1 is the weighting factor for consolidation; C_2 is the weighting factor for degradation. The optimization procedure used for the resistance welding process is illustrated in Figure 4. Here, I is the applied current intensity (A); w is the width of the heating element (m); and t_h is the heating time during which power is supplied (s). Using the Nelder–Mead method, values for the controllable process variables (I and t_h) are determined leading to minimum processing time, t_w . The Nelder–Mead algorithm proceeds from three initial values of the objective function because the number of variables is two, I_w and t_h , and then calculates the next iteration values. At the start of the optimization, initial values of the weighting factors are taken as 10 and 1000, respectively. These low values are chosen to preclude the penalty terms getting very large values during the initial stages of the optimization where severe constraint violations are possible.

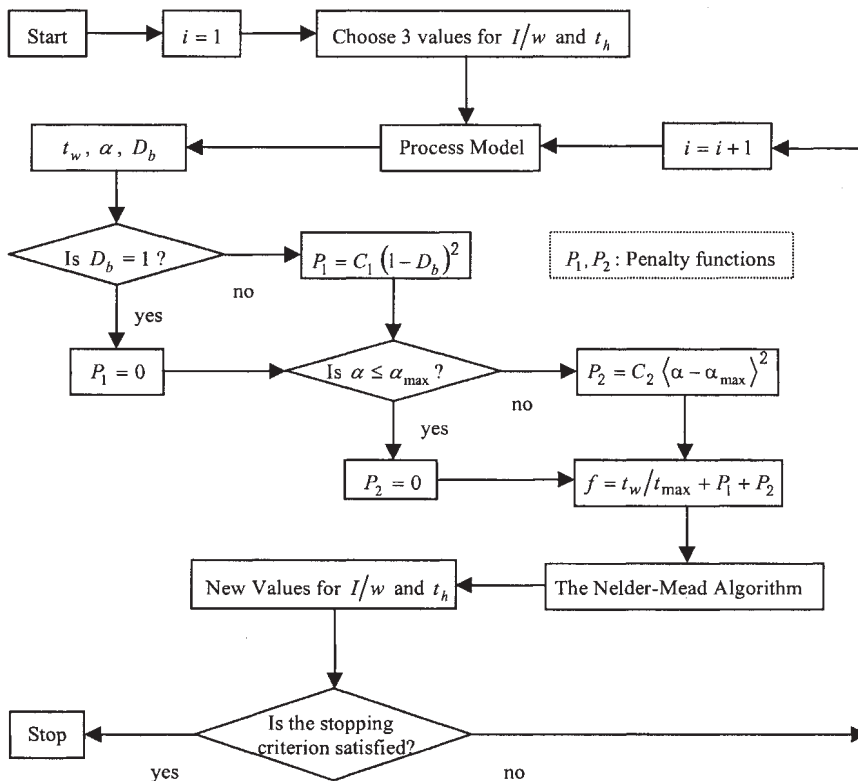


Figure 4. The optimization procedure for the resistance welding process.

During optimization, these values are increased in each iteration until they reach a certain limit. Their limiting values are 1×10^6 and 1×10^{12} , respectively. These values are appropriate in the sense that if lower values are chosen, the solution may not converge to a point within the feasible region or very close to it, but to a point that can be considered to be too far from the feasible region. On the other hand, if higher values are used, the solution will not improve.

RESULTS AND DISCUSSIONS

Verification

Validation of the numerical models is essential for their reliable use. For this reason, the numerical heat transfer model was verified by comparing the numerical results for a simpler problem to an available analytical solution. Özisik [36], using the orthogonal expansion technique, obtained the analytical solution of the time-dependent heat conduction equation for a composite medium with heat generation. The benchmark problem is schematically illustrated in Figure 5(a). We assumed that the first layer consists of APC-2, whereas the second layer consists of PEEK. There was heat generation within the first layer at a constant rate of $\dot{q}(W/m^3)$. The outer boundary at $x=0$ is kept insulated. The boundary surface at $x=x_2$ dissipates heat by convection into the surrounding air with the heat transfer coefficient $h=5\text{ W/m}^2\text{ }^\circ\text{C}$. Because of the restriction of the analytical method, constant thermal coefficients were used, which correspond to those at 250°C [2]. Input parameters of the problem are given in Table 1, where T_{ini} is the initial temperature.

The analytical solution of the benchmark problem is compared with its numerical solution in Figure 5(b). The relative error at the maximum temperature is 1.14%, indicating a good agreement between the analytical and the numerical results.

The accuracy of the process model predictions was examined by comparing them with the experimentally determined interlaminar shear strengths of specimens joined by resistance welding. A convenient way of characterizing the quality of the joint is through

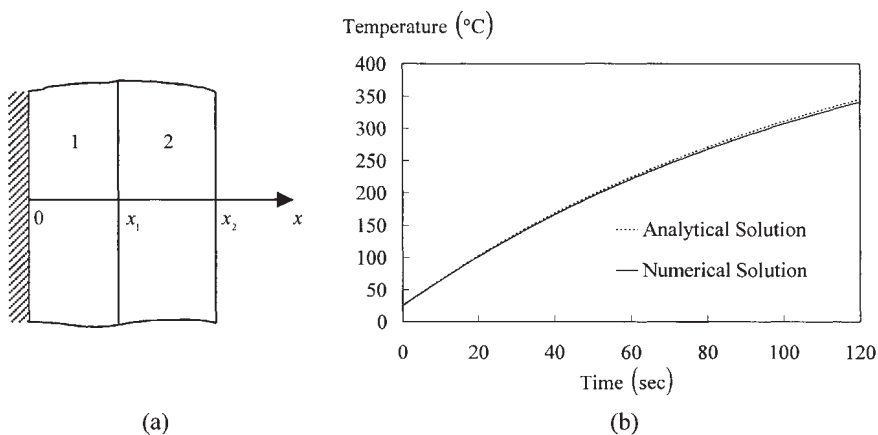


Figure 5. (a) Transient conduction through a two-layer composite region; (b) temperature variation at $x=0$.

Table 1. Input parameters for the simplified problem.

I/w (A/m)	X_1 (mm)	X_2 (mm)	Δx (mm)	T (°C)	T_{int} (°C)
120	0.127	0.254	0.0127	23	25

Table 2. Comparisons of the degrees of bonding obtained using the model, and the shear strength ratios obtained experimentally.

\dot{q} (kW/m ²)	t_h (sec)	σ (MPa)	σ/σ_∞	D_b
52	225	42.1	0.64	0.72
71	116	39.4	0.60	0.63
71	124	44.8	0.68	0.69

measuring the bond strength. Don et al. [1,12] experimentally investigated fusion bonding of two 16-ply APC-2 laminates by resistance welding. At the joint, they used a heating element sandwiched between two layers of neat PEEK film, and experimentally quantified the influence of processing time and power input on the performance of the joint through lap-shear testing. Using the same process parameters, the strengths of the welded joints were numerically quantified by the present process model. The values for the degree of bonding were calculated by Equation (22). The comparison of the numerical results and the experimental data reported by Don et al. is given in Table 2. Here, \dot{q} is the power level; and t_h is the heating time during which the current is applied. The calculated values for the degree of bonding, D_b , and the measured values of σ/σ_∞ , which is the ratio of the measured shear strengths to the ultimate shear strengths, are in good agreement. The ultimate lap-shear strength for APC-2 was reported to be 65.55 MPa [37].

Processing Windows

Using the process model, a parametric study was conducted in order to observe the feasible range of controllable process variables, which were the current intensity, I/w , and heating time, t_h . The results are shown in Figures 6 and 7. As seen in these figures, the feasible area for the controllable process variables consists of a narrow band. Increasing heating time or current intensity may result in excessive degradation. Decreasing them may lead to insufficient consolidation. Therefore, one should be careful in choosing appropriate values for the variables during the resistance welding process.

Minimum Processing Times

Using the Nelder–Mead method [34], optimum values for controllable process variables were calculated. As given by Don et al. [1,12], the thickness of the ceramic insulator was taken as 2.5 cm. The material properties of the ceramic insulator are given in Table 3. The heat transfer coefficient, h , for the still air was given by Cogswell [31]

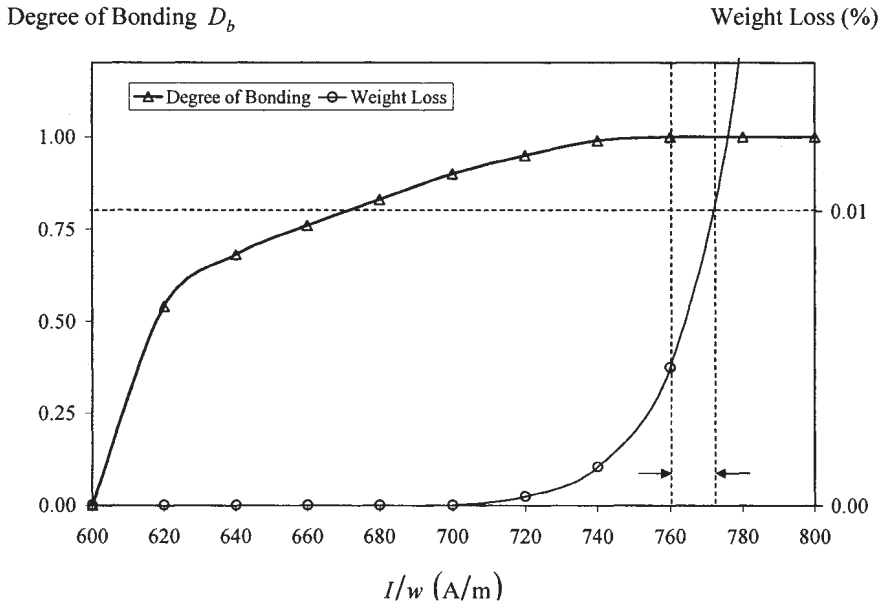


Figure 6. Joining 16-ply APC-2 laminates with constant heating time $t_h = 120$ s.

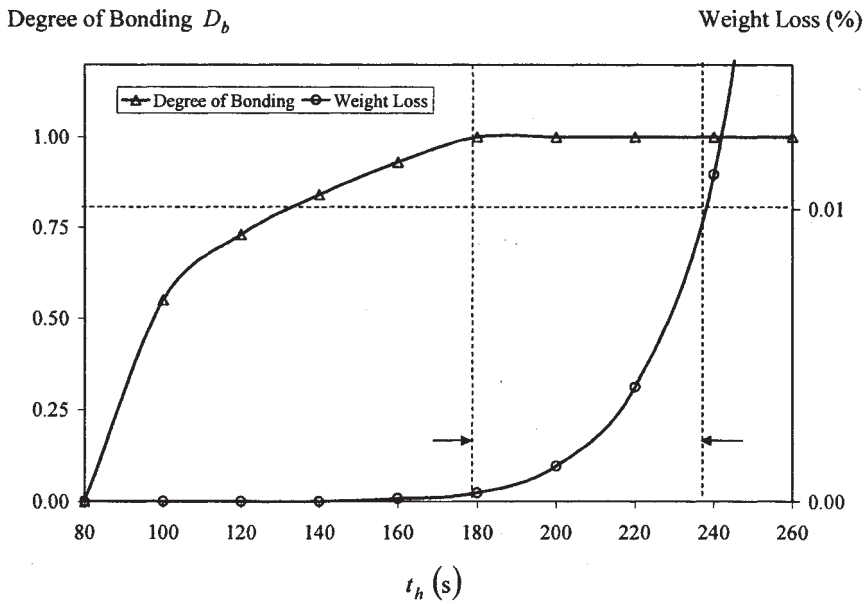


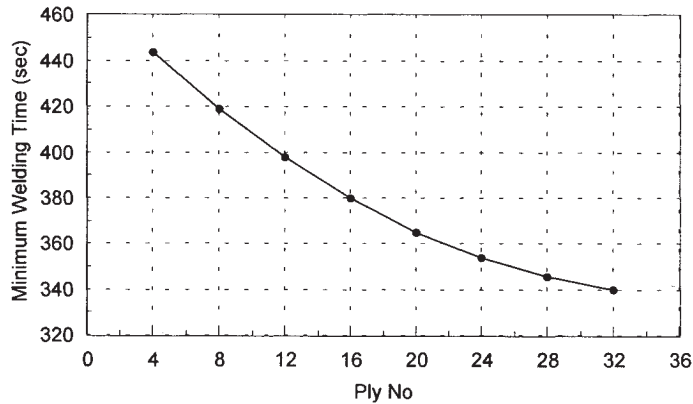
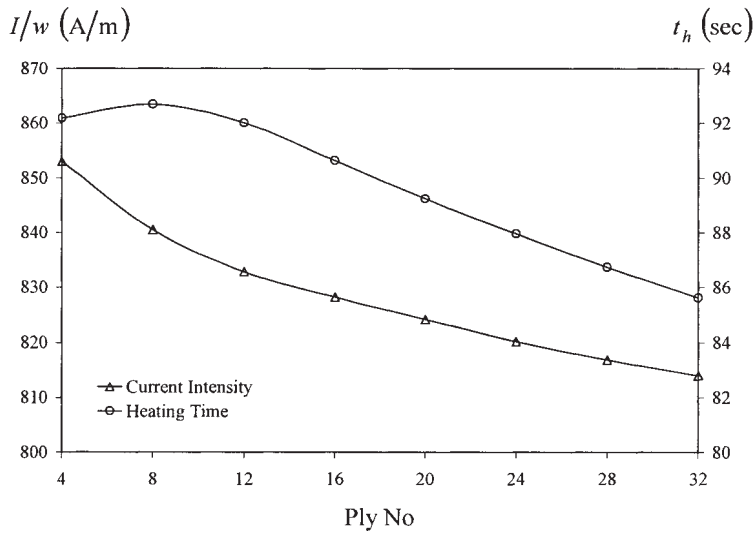
Figure 7. Joining 16-ply APC-2 laminates with constant heating time $I/w = 666$ A/m.

as $10 \text{ W/m}^2\text{ }^\circ\text{C}$. The obtained results for different APC-2 laminate thicknesses are illustrated in Figures 8 and 9.

For each laminate thickness, the optimization algorithm was employed about 20 times using randomly chosen initial values for the process parameters. Nearly 80% of times, the

Table 3. Material property data for the pressure plates [38].

	Ceramic	Steel	Aluminum
k , conductivity (W/m°C)	1	45	210
C , specific heat (J/kg°C)	830	473	896
ρ , density (kg/m ³)	2600	7800	2707

**Figure 8.** Minimum welding times, t_w , for different laminate thicknesses.**Figure 9.** Corresponding optimum process parameters.

algorithm converged to the same value of local minimum. Also, the corresponding degrees of degradation were very close to the allowable amount of degradation. These observations assure us that the results represent the global minimum of the objective function.

As the thickness of the APC-2 laminate is increased, which has lower transverse conductivity than that of the ceramic insulator, heat loss becomes more difficult. For this

reason, for a thick laminate less power is needed to achieve consolidation. Even if the current intensity is lower for the thicker laminates, the rate of temperature increase is higher as seen in Figure 10, which shows the resulting change of temperature with time at the center of the heating element when the optimum process parameters corresponding to 4-, 16- and 32-ply APC-2 laminates are used. Paradoxically, cooling is also fast. Cooling occurs mainly due to conduction heat transfer from the heated element to the cooler (unheated) parts. When the volume of the unheated parts is larger because of thicker laminate, the increase in their temperature through heat conduction becomes smaller due to their increased heat capacity ($J/^\circ C$). Consequently, temperature difference between heated and unheated parts becomes larger, and thus heat transfer (and cooling) rate increases.

Figure 11 shows the variation of minimum welding times, t_w , for different thicknesses of ceramic insulator. When it is thin, welding times are very long. The reason lies in the

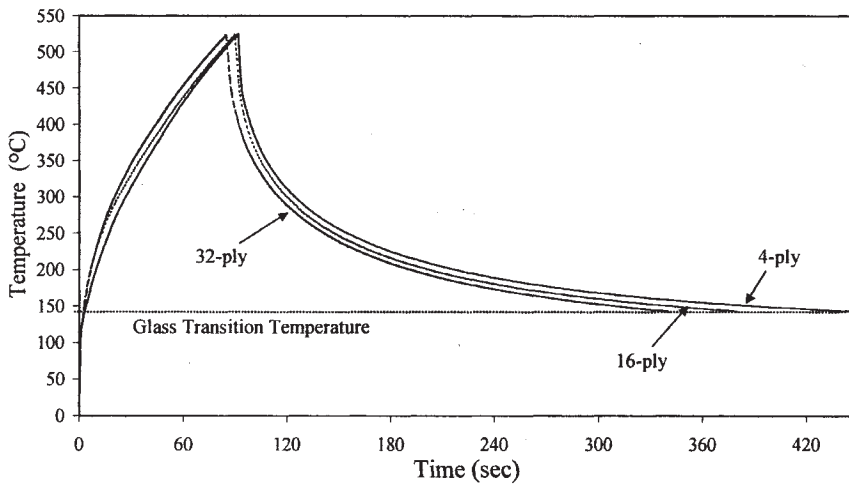


Figure 10. Temperature variation at the center of the heating element during welding with the optimum process parameters of 4-, 16- and 32-ply APC-2 laminates.

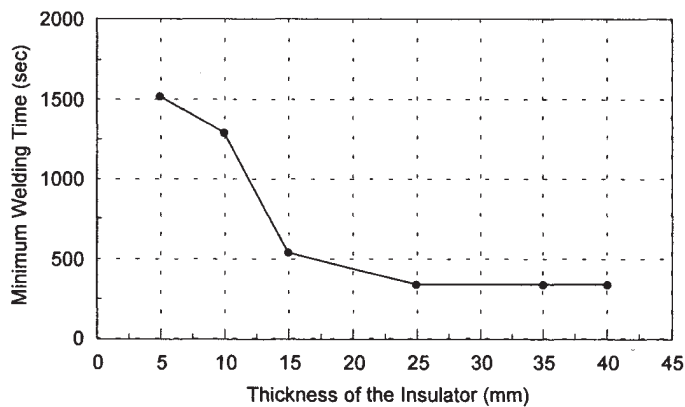


Figure 11. Minimum welding times, t_w for different thicknesses of ceramic insulator. Laminate contains 32 plies.

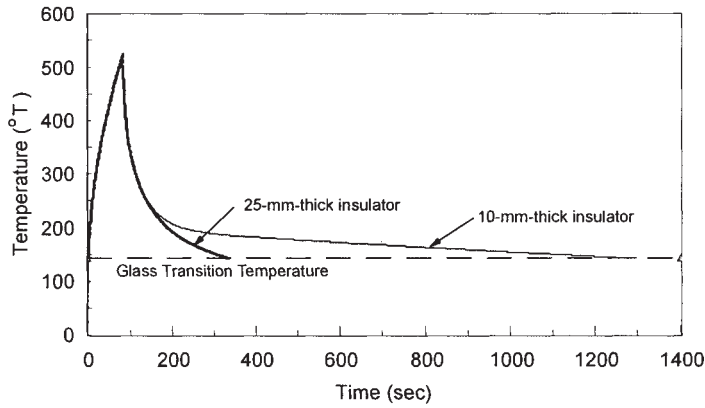


Figure 12. Temperature variation at the center of the heating element during welding corresponding to different ceramic insulator thicknesses.

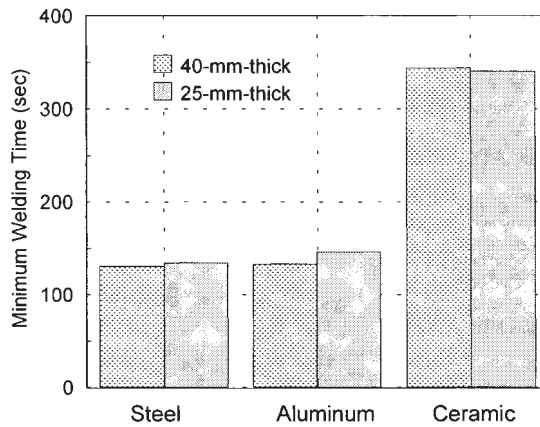


Figure 13. Minimum welding times, t_w corresponding to the cases where different materials are used for the pressure plates. Laminate contains 32 plies.

reduced heat capacity ($J/^\circ C$), which leads to large increases in the temperature of the insulator during welding. This could even be higher than the glass transition temperature. Cooling then can only be achieved through heat loss to the air, which is a very slow process (Figure 12). On the other hand, when the insulator is thick, main cooling mechanism is heat conduction throughout the welding process. Therefore, cooling time, and thus process time, is shorter. However, further increase in thickness beyond a certain limit does not reduce the welding time. If the thickness of the ceramic insulator is greater than 25 mm, it does not experience any significant temperature rise, and consequently increase in its thickness does not affect the cooling rate.

The resistance welding process can be achieved using pressure plates made of metal instead of using ceramic insulator. As Figure 13 shows, metal plates lead to shorter welding times. This is because they provide more effective cooling, but at the expense of a higher requirement regarding current intensity and heating time ($I/w=888$ A/m and $t_h=94$ s for steel as opposed to $I/w=814$ A/m and $t_h=86$ s for ceramic). In comparison to

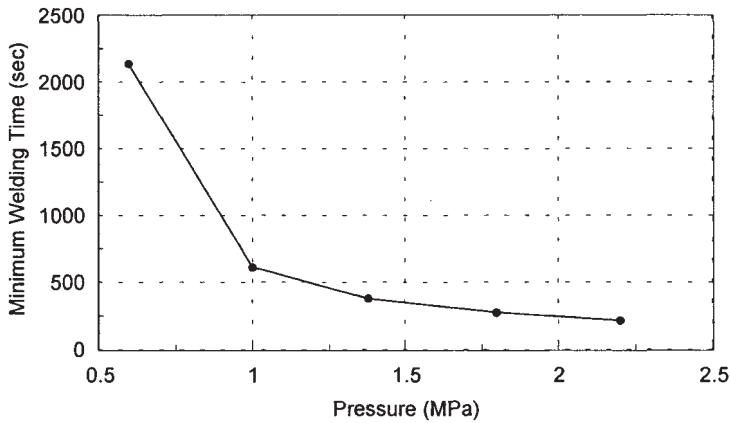


Figure 14. Minimum welding times, t_w corresponding to different values of applied pressure. Laminate contains 16 plies.

aluminum, steel would be a better choice because of its higher heat capacity per unit volume ($J/^\circ C m^3$).

Figure 14 depicts the variation of minimum welding time with pressure. If the applied pressure is low, full consolidation becomes more difficult and a longer dwell time at high temperatures is required. This can be achieved by increasing the heating time, but also reducing the current intensity in order not to cause degradation. Consequently, welding time would be longer. On the other hand, when the pressure is increased, consolidation can sooner be achieved. ($I/w=651$ A/m and $t_h=236$ s for $P=0.6$ MPa, as opposed to $I/w=892$ A/m and $t_h=67$ s for $P=1.8$ MPa.) However, after a certain limit this effect subsides.

Crystallinity of a semi-crystalline polymer is known to affect its mechanical properties. Recommended levels of crystallinity for APC-2 are between 25 and 35% [31]. According to the experimental data of Velisaris and Seferis [39] and Talbott et al. [40], cooling rates between 10 and $100^\circ C/min$ result in recommended levels of crystallinity. The experimental data given by Motz and Schultz [33] showed that crystallization phenomenon approximately occurs between temperatures of 320 and $160^\circ C$. As seen in Figure 10, cooling rates are about $50\text{--}60^\circ C$ within this temperature range. Therefore, crystallinity levels corresponding to optimum process parameters are expected to be within recommended levels.

CONCLUSIONS

In this study, process modeling of resistance welding for thermoplastic composites was carried out. Heat transfer, degradation kinetics and consolidation models were developed, and then combined to establish the process window, which is defined as the feasible ranges of the controllable process parameters. The optimization method, called Nelder–Mead, was employed in order to determine the process parameters, which resulted in the minimum processing time with desired quality of the welded joint. The controllable process parameters were the current intensity and the heating time. For different thicknesses of APC-2 laminates, the optimum process parameters and corresponding

welding times were found. As the thickness of the APC-2 laminate was increased, the power requirement reduced, and welding times decreased. Thickness of the insulator was found to affect the welding time. Very thin plates should be avoided since they lead to quite long welding times. Use of steel plates instead of ceramic insulator was advised. Welding can then be achieved in a very short time. Applied pressure should not be low, but also should not be unnecessarily high.

ACKNOWLEDGMENT

This paper is based on the work supported by the Research Fund of Bogazici University with the code number 97HA602.

REFERENCES

1. Don, R.C., Gillespie, J.W., Jr. and Lambing, C.L.T. (1992). Experimental characterization of processing-performance relationships of resistance welded graphite/polyetherether-ketone composite joints. *Polymer Engineering and Science*, **32**(9): 620–631.
2. Ageorges, C., Ye, L., Mai, Y.-W. and Hou, M. (1998). Characteristics of resistance welding of lap shear coupons. Part I: heat transfer. *Composites Part A*, **29**(8): 899–909.
3. Hou, M., Yang, M., Beehag, A., Mai, Y.-W. and Ye, L. (1999). Resistance welding of carbon fibre reinforced thermoplastic composite using alternative heating element. *Composite Structures*, **47**: 667–672.
4. Smiley, A.J., Halbritter, A., Cogswell, F.N. and Meakin, P.J. (1991). Dual polymer bonding of thermoplastic composite structures. *Polymer Engineering and Science*, **31**(7): 526–532.
5. Xiao, X.R., Hoa, S.V., and Street, K.N. (1992). Processing and modelling of resistance welding of APC-2 composite. *Journal of Composite Materials*, **26**(7): 1031–1049.
6. Benatar, A. and Gutowski, T.G. (1986). Methods for fusion bonding thermoplastic composites. *SAMPE Quarterly*, **18**(1): 35–41.
7. Eveno, E.C. and Gillespie, J.W., Jr. (1988). Resistance welding of graphite polyetheretherketone composites: an experimental investigation. *Journal of Thermoplastic Composite Materials*, **1**: 322–338.
8. Maffezzoli, A.M., Kenny, J.M. and Nicolais, L. (1989). Welding of PEEK/carbon fiber composite laminates. *SAMPE Journal*, **25**(1): 35–39.
9. Jakobsen, T.B., Don, R.C. and Gillespie, J.W., Jr. (1989). Two-dimensional thermal analysis of resistance welded thermoplastic composites. *Polymer Engineering and Science*, **29**(23): 1722–1729.
10. Bastien, L.J. and Gillespie, J.W., Jr. (1991). A non-isothermal healing model for strength and toughness of fusion bonded joints of amorphous thermoplastics. *Polymer Engineering and Science*, **31**(24): 1720–1730.
11. Holmes, S.T. and Gillespie, J.W., Jr. (1992). Thermal analysis for resistance welding of large-scale thermoplastic composite joints. In: *Proceedings of the American Society for Composites 7th Technical Conference*. Lancaster, PA: Technomic Publishing Co., pp. 135–146.
12. Don, R.C., Bastien, L., Jakobsen, T.B. and Gillespie, J.W., Jr. (1990). Fusion bonding of thermoplastic composites by resistance heating. *SAMPE Journal*, **26**(1): 59–66.
13. Hou, M., Ye, L. and Mai, Y.-W. (1999). An experimental study of resistance welding of carbon fibre fabric reinforced polyetherimide (CF fabric/PEI) composite material. *Applied Composite Materials*, **6**: 35–49.
14. Ageorges, C., Ye, L., Mai, Y.-W. and Hou, M. (1998). Characteristics of resistance welding of lap shear coupons. Part II: consolidation. *Composites Part A*, **29**(8): 911–919.

15. Ageorges, C., Ye, L., Mai, Y.-W. and Hou, M. (1998). Characteristics of resistance welding of lap shear coupons. Part III: crystallinity. *Composites Part A*, **29**(8): 921–932.
16. Özisik, M.N. (1993). *Heat Conduction*. New York: John Wiley.
17. Day, M., Cooney, J.D. and Wiles, D.M. (1989). The kinetics of the oxidative degradation of poly(aryl-ether-ether-ketone) (PEEK). *Thermochimica Acta*, **147**(1): 189–197.
18. Pitchumani, R., Gillespie, J.W., Jr. and Lamontia, M.A. (1997). Design and optimization of a thermoplastic tow-placement process with in-situ consolidation. *Journal of Composite Materials*, **31**(3): 244–275.
19. Nam, J.-D. and Seferis, J.C. (1992). Generalized composite degradation kinetics for polymeric systems under isothermal and nonisothermal conditions. *Journal of Polymer Science: Part B (Polymer Physics)*, **30**(5): 455–463.
20. Bowles, K.J. and Frimpong, S. (1992). Void effects on the interlaminar shear strength of unidirectional graphite-fiber-reinforced composites. *Journal of Composite Materials*, **26**(10): 1487–1509.
21. Loos, A.C. and Dara, P.H. (1987). Processing of thermoplastic matrix composites. *Review of Progress in Quantitative Nondestructive Evaluation*, **6B**: 1257–1265.
22. Lee, W.I. and Springer, G.S. (1987). A model of the manufacturing process of thermoplastic matrix composites. *Journal of Composite Materials*, **21**(11): 1017–1055.
23. Mantell, S.C. and Springer, G.S. (1992). Manufacturing process models for thermoplastic composites. *Journal of Composite Materials*, **26**(16): 2348–2377.
24. De Gennes, P.G. (1971). Reptation of a polymer chain in the presence of fixed obstacles. *Journal of Chemical Physics*, **55**(2): 572–579.
25. Wool, R.P. and O'Connor, K.M. (1981). A theory of crack healing in polymers. *Journal of Applied Physics*, **52**(10): 5953–5963.
26. Kim, Y.H. and Wool, R.P. (1983). A theory of healing at a polymer–polymer interface. *Macromolecules*, **16**(7): 1115–1120.
27. Cho, B.-R. and Kardos, J.L. (1995). Consolidation and self-bonding in poly(ether ether ketone) (PEEK). *Journal of Applied Polymer Science*, **56**: 1435–1454.
28. Sonmez, F.O. and Hahn, H.T. (1997). Analysis of the on-line consolidation process in thermoplastic composite tape placement. *Journal of Thermoplastic Composite Materials*, **10**(6): 543–572.
29. Colak, Z.S. (2000). Process modeling of resistance welding for thermoplastic composites. M.S. Thesis, Department of Mechanical Engineering, Bogazici University, Istanbul.
30. Pitchumani, R., Ranganathan, S., Don, R.C., Gillespie, J.W., Jr. and Lamontia, M.A. (1996). Analysis of transport phenomena governing interfacial bonding and void dynamics during thermoplastic tow-placement. *International Journal of Heat and Mass Transfer*, **39**(9): 1883–1897.
31. Cogswell, F.N. (1992). *Thermoplastic Aromatic Polymer Composites*. Butterworth-Heinemann Ltd.
32. Sonmez, F.O. and Hahn, H.T. (1997). Process modeling of heat transfer and crystallization for thermoplastic composite tape placement. *Journal of Thermoplastic Composite Materials*, **10**(3): 198–240.
33. Motz, H. and Schultz, J.M. (1989). The solidification of PEEK. Part II: kinetics. *Journal of Thermoplastic Composite Materials*, **2**: 267–279.
34. Nelder, J.A. and Mead, R. (1965). A simplex method for function minimization. *Computer Journal*, **7**(4): 308–313.
35. Siddall, J.N. (1982). *Optimal Engineering Design: Principles and Applications*. New York: Marcel Dekker.
36. Özisik, M.N. (1968). *Boundary Value Problems of Heat Conduction*. Scranton: International Textbook Co.
37. Mantell S.C., Wang, Q. and Springer, G.S. (1992). Processing thermoplastic composites in a press and by tape laying experimental results. *Journal of Composite Materials*, **26**(16): 2378–2401.

38. Geankoplis, C.J. (1983). *Transport Processes and Unit Operations*. Allyn and Bacon Inc.
39. Velisaris, C.N. and Seferis, J.C. (1986). Crystallization kinetics of polyetheretherketone (PEEK) matrices. *Polymer Engineering and Science*, **26**(22): 1574–1581.
40. Talbott, M.F., Springer, G.S., and Berglund, L.A. (1987). The effects of crystallization on the mechanical properties of PEEK polymer and graphite fiber reinforced PEEK. *Journal of Composite Materials*, **21**: 1056–1081.